Associations between locus coeruleus integrity and diagnosis, age, and cognitive performance in older adults with and without late-life depression: An exploratory study

Navona Calarco [a], Clifford M. Cassidy [b], Ben Selby [a], Colin Hawco [a], Aristotle N. Voineskos [a,c], Breno S. Diniz [d,e], Yuliya S. Nikolova [a,c,*]

[a] Campbell Family Mental Health Research Institute, Centre for Addiction and Mental Health (CAMH), Toronto, ON, Canada
[b] The University of Ottawa Institute of Mental Health Research at the Royal, Ottawa, ON, Canada
[c] Department of Psychiatry, University of Toronto, Toronto, ON, Canada
[d] UConn Center on Aging, University of Connecticut Health Center, Farmington, CT, USA
[e] Department of Psychiatry, School of Medicine, University of Connecticut, Farmington, CT, USA

A R T I C L E   I N F O

A B S T R A C T

Late-life depression (LLD) is a risk factor for age-dependent cognitive deterioration. Norepinephrine-related degeneration in the locus coeruleus (LC) may explain this link. To examine the LC norepinephrine system in vivo, we acquired neuromelanin-sensitive MRI (NM-MRI) in a sample of 48 participants, including 25 with LLD (18 women, age 68.08 ± 5.41) and 23 never-depressed comparison participants (ND, 12 women, age 70 ± 8.02), matched on age and cognitive status. We employed a semi-automated procedure to segment the LC into three bilateral sections along its rostro-caudal extent, and calculated relative contrast as a proxy of integrity. Then, we examined associations between integrity and LLD diagnosis, age, and cognition, as measured via the Repeatable Battery for the Assessment of Neuropsychological Status (RBANS) and the Delis-Kaplan Executive Function System (D-KEFS). We did not identify an effect of LLD diagnosis nor age on LC integrity, but exploratory canonical correlation analysis across the combined participant sample revealed a strong (Rc = 0.853) and significant multivariate relationship between integrity and cognition (Wilks' $\lambda = 0.03$, $F(84, 162.44) = 1.66$, $p = <.01$). The first and only significant variate explained 72.83% model variance, and linked better attention and delayed memory performance, faster processing speed, and lower verbal fluency performance with higher integrity in the right rostral but lower integrity in the left caudal LC. Our results complement prior evidence of LC involvement in cognition in healthy older adults, and extend this association to individuals with LLD.

1. Introduction

Major depressive disorder (MDD), particularly when experienced in late life (i.e., late-life depression or LLD), is associated with elevated risk of subsequent cognitive decline and dementia (Byers and Yaffe, 2011). The biological mechanisms underlying this association remain poorly understood, but converging lines of evidence implicate the degeneration of the locus coeruleus (LC), a small brainstem nucleus adjacent to the lateral floor of the fourth ventricle that is the largest source of norepinephrine in the human brain (Schwarz and Luo, 2015). Postmortem

cellular and molecular pathology studies suggest that the neurodegeneration of norepinephrine projections originating in the LC may represent a shared biological mechanism underlying MDD and age-dependent cognitive decline. Norepinephrine dysfunction is common in MDD at any age (Anand and Charney, 2000; Cottingham and Wang, 2012) and is associated with deficits in cognitive flexibility, attention and memory (Chamberlain and Robbins, 2013). The LC is among the first regions to show neuronal degeneration as a function of normal aging, and LC pathology is evident in several neurodegenerative conditions marked by cognitive impairment, including Alzheimer's disease

(Beardmore et al., 2021). Additional postmortem studies, albeit in very small samples, suggest that age-dependent degenerative processes in the LC may be accelerated or accentuated in older individuals with chronic depression, even in the absence of dementia (Chan-Palay and Asan, 1989).

Recent progress in magnetic resonance imaging (MRI) allows measurement of the LC-norepinephrine system in vivo, variably termed neuromelanin-sensitive MRI (NM-MRI) (Sasaki et al., 2006), LC-MRI (Keren et al., 2015), or magnetization transfer MRI (MT-MRI) (Priovoulos et al., 2020). NM-MRI yields high signal contrast in the LC, allowing for it to be visually distinguished from surrounding tissue. Though the physical mechanisms underlying NM-MRI contrast are subject to active debate (Trujillo et al., 2017; Kelberman et al., 2020), it is believed to reflect features of norepinephrine neurons, including levels of neuromelanin (Keren et al., 2015) and intracellular water content (Watanabe et al., 2019). Thus, signal contrast, typically relative to a reference region, is taken as a proxy measure of neuronal "integrity". Reduced relative contrast in the LC has been shown to be associated with smaller LC volume (Keren et al., 2015) and fewer norepinephrine terminals (Sommerauer et al., 2018).

A burgeoning body of work has probed the ability of LC-MRI (henceforth used to indicate NM-MRI in the LC) to detect pathology in a variety of neurodegenerative diseases (Betts et al., 2019; Liu et al., 2017), as well as healthy aging and cognition. A near-consensus has found LC integrity to predict performance in a variety of cognitive domains, including cognitive reserve (Clewett et al., 2016), memory (Dahl et al., 2019; Hämmerer et al., 2018), and global cognitive ability (Liu et al., 2020b), with recent studies suggesting associations to be particularly pronounced in rostral LC (Liu et al., 2020b; Dahl et al., 2019). Studies of healthy aging and LC-MRI are more mixed, but lifespan studies tend to suggest that LC-MRI signal takes an inverted-U shape along chronological age, peaking around mid-life and slightly decreasing, or in some studies plateauing, in individuals > 60 years old (Shibata et al., 2006; Liu et al., 2019). To date, only a small number of studies have examined LC-MRI in depression. These studies have reported reduced LC integrity in individuals with depression relative to healthy controls, both in middle age (Shibata et al., 2008, 2007) and late-life (Guinea-Izquierdo et al., 2021), in general agreement with earlier post-mortem investigation (Chan-Palay and Asan 1989). Thus, considered together, it seems that high levels of relative LC-MRI contrast are neuroprotective against age-related cognitive decline in health and disease, including depression.

Here, we set out to investigate if MR-indexed LC integrity might constitute a biomarker of depression in older adults, over and above associations with aging and cognition. Following evidence that the LC may have a topographical arrangement, with non-homogeneous structure (Beardmore et al., 2021) and connections (Poe et al., 2020) that may be functionally dissociable (Dahl et al., 2019), we examined LC integrity in three bilateral rostral-caudal sections. Then, we tested independent and interactive effects of LLD diagnosis and age, and multivariate associations to cognition. In keeping with prior literature, we hypothesized that we would observe lower LC integrity in the LLD group compared to never-depressed (ND) comparison participants. Further, we hypothesized that LC integrity might slightly decline as a function of age, though all participants in our sample were >60 years old. Lastly, we hypothesized that, in both individuals with and without LLD, LC integrity would be strongly associated with cognitive performance.

2. Materials and methods

2.1. Eligibility criteria

Participants aged 60–85 were recruited from the Centre for Addiction and Mental Health (CAMH) in Toronto via advertisements, word of mouth, and the hospital research registry; participants with LLD were also recruited from within the Geriatric Psychiatry clinic. All LLD participants met DSM-5 diagnostic criteria for a current major depressive episode (MDE), confirmed by the Depression and Manic Episode Modules (A and C) on the MINI-International Neuropsychiatric Interview (Sheehan et al., 1998). LLD participants had no current or past history of other major psychiatric disorders. We included a never-depressed (ND) comparison group without a current or past history of any Axis I psychiatric disorder. Neither LLD nor ND participants showed evidence of probable cognitive impairment or dementia as determined by a score less than 22 on the Montreal Cognitive Assessment (MoCA) (Nasreddine et al., 2005). LLD and ND participants were excluded for substance abuse or dependence (past six months, excluding tobacco), any contraindication to MRI, intellectual disability, severe head trauma, stroke, other neurodegenerative disorders, and current unstable medical illness. All participants provided written informed consent. The protocol was approved by the CAMH Research Ethics Board and conducted following the Declaration of Helsinki.

2.2. Participant sample

Demographic and clinical characteristics for the final sample of n = 48, including 25 LLD (18 women, age 68.08 ± 5.41 years), and 23 ND comparison participants (12 women, age 70 ± 8.02 years), are reported in Table 1. Seventeen LLD participants reported recurrent MDE, five reported past MDE, and three were experiencing a first MDE. Thirteen LLD participants were on antidepressant medication(s) at the time of MR imaging. As medications with norepinephrine targets may affect LC signal intensity (Guinea-Izquierdo et al., 2021), we conducted sensitivity analyses without the four LLD participants taking noradrenergic medication for depression (i.e., serotonin and norepinephrine reuptake inhibitors (SNRIs), norepinephrine and dopamine reuptake inhibitor (NDRIs), noradrenergic and specific serotonergic antidepressants (NaSSAs), or Tricyclics) (see Inline Supplementary Table 1), and/or the five participants (2 ND, 3 LLD) taking noradrenergic antagonist medication (i.e., beta-blockers) for other indications (see Inline Supplementary Table 2). As the exclusion of participants taking medications with norepinephrine targets did not meaningfully change results, and medication type was independent of LC-MRI contrast ratio (p=.66), we present results from the whole sample.

2.3. Cognitive assessment

Cognition was assessed using the Repeatable Battery for the Assessment of Neuropsychological Status (RBANS) (Randolph et al., 1998) and the Delis-Kaplan Executive Function System (D-KEFS) (Delis 2001). The RBANS evaluates performance in principal cognitive domains, namely attention, memory (immediate and delayed), language, and visuospatial ability. The D-KEFS includes the Color-Word Interference Task (CWIT; color naming, word reading, inhibition, and inhibition/switching), the Trail Making Test (TMT; numbers and number-letter switching), and the Verbal Fluency task (letter fluency, category fluency, and category switching). In total, we collected 14 independent measures of cognitive performance (see Table 1).

2.4. Magnetic resonance imaging

2.4.1. Image acquisition

All MR images were acquired on a Siemens 3 T Prisma (Siemens Medical Solutions, Malvern, PA, USA), using a 64-channel head coil. NM-MRI was acquired with a 2D gradient-recalled echo (GRE) sequence with an explicit MT contrast preparation pulse placed prior to the excitation pulse. Acquisition parameters were in general keeping with previously published protocols for the simultaneous imaging of the LC and the substantia nigra (Chen et al., 2014), which produce reproducible contrast ratio measurements (Langley et al., 2017; Wengler et al., 2020b), and estimates of volume (Langley et al., 2017). Parameters were as follows: repetition time (TR) = 389 ms, echo time (TE) = 2.9 ms, flip

Table 1
Participant Characteristics.

	LLD n = 25	ND n = 23	Statistic (p value)
Demographic characteristics			
Age	68.08 (5.41)	70.00 (8.02)	0.34
Sex (Female:Male)	18:7	12:11	0.26
Clinical characteristics			
Montreal Cognitive Assessment (MoCA)	26.30 (2.01)	26.08 (2.52)	0.73
Patient Health Questionnaire (PHQ-9)	12.28 (4.31)	0.78 (1.28)	<0.001
Montgomery-Asberg Depression Rating Scale (MADRS)	16.60 (5.69)	1.00 (1.41)	<0.001
Repeatable Battery for the Assessment of Neuropsychological Status (RBANS)			
Immediate memory	98.48 (13.29)	96.43 (12.43)	0.58
Visuospatial / constructional	92.68 (17.30)	97.17 (15.80)	0.35
Language	99.64 (9.33)	98.87 (12.52)	0.81
Attention	101.24 (16.43)	107.17 (16.89)	0.22
Delayed memory	100.96 (11.08)	97.00 (14.89)	0.31
Delis-Kaplan Executive Function System (D-KEFS)			
Trail Making Test: Numbers	41.24 (14.30)	41.57 (28.43)	0.96
Trail Making Test: Numbers-letters	122.68 (59.00)	105.43 (47.96)	0.27
Color-Word Interference Test – 1: Colour naming	34.16 (10.35)	34.22 (6.99)	0.98
Color-Word Interference Test – 2: Word reading	24.28 (6.36)	25.52 (5.53)	0.47
Color-Word Interference Test – 3: Inhibition	68.12 (23.45)	62.39 (16.78)	0.33
Color-Word Interference Test – 4: Inhibition / switching	68.68 (22.03)	64.43 (11.97)	0.41
Verbal fluency: Letters	40.92 (11.97)	42.52 (11.45)	0.64
Verbal fluency: Categories	39.44 (7.95)	37.57 (9.61)	0.47
Verbal fluency: Category switching	13.36 (2.97)	13.22 (3.36)	0.88

Values in table represent mean (SD). P values derive from Student's t-tests or Chi-squared tests, as appropriate. There were no differences in group demographic characteristics, cognitive status (MoCA adjusted for education), or cognition. Note that the two D-KEFS Trail Making Test scores and the four D-KEFS Colour-Word Interference Test scores are time-to-completion (seconds); thus, lower scores are better. As expected, the late-life depression (LLD) group showed statistically higher ratings than the comparison (ND) group on the PHQ-9 and MADRS assessments of depression.

angle = 40°, in-plane resolution = 0.39 × 0.39 mm, partial brain coverage with field of view (FOV) = 124.8 mm × 200 mm, acquisition matrix = 512 × 416, slice thickness = 3 mm, slice gap = 0 mm, number of slices = 15, MT frequency offset = 1200 Hz, MT flip angle = 300°, number of signal averages = 4, acquisition time = ~10 min, default reference voltage scaling. The 15 contiguous slices were positioned perpendicular to the dorsal edge of the brainstem starting from the lower pons, i.e., below the most caudal extent of the LC. We also acquired high-resolution, whole-brain T1- and T2-weighted structural scans in the same session (see Inline Supplementary Table 3 for parameters). Prior to image processing, we performed multilayer quality control of the NM, T1, and T2 images. Specifically, we (i) verified scans were acquired with the parameters described above, (ii) reviewed quantitative metrics indicative of scan quality (e.g., signal-to-noise, contrast-to-noise) and

(iii) ensured no artifacts that might affect our LC segmentation method (ghosting, blurring) were discernible by eye. The final sample of n = 48 excludes one participant with suboptimal slab placement on NM-MRI. Motion was estimated by framewise displacement, i.e., the transform (mm) required for the alignment of the four NM images. A *t*-test comparing motion between the LLD (M = 0.74, SD = 0.44) and ND (M = 0.68, SD = 0.40) groups found no statistical difference, $p = .61$, d = 0.15.

2.4.2. LC segmentation approach

We segmented the LC via a previously described "funnel-tip" method (Cassidy et al., 2022). This semi-automated method segments in each participants' native space, via an (automated) intensity-threshold-free cluster search within an (manually-drawn) overinclusive mask. Several recent papers have also opted to segment in native space (Jacobs et al., 2021; Olivieri et al., 2019; Giorgi et al., 2022a, b; García-Lorenzo et al., 2013), which obviates the distortion that can be introduced via registration to a template, which can be especially threatening to small structures. However, our overinclusive mask showed high overlap with the recently published "metaMask" template (Dahl et al., 2022), which averages six previously published LC masks (Betts et al., 2017; Dahl et al., 2019; Keren et al., 2009; Liu et al., 2019; Tona et al., 2017; Ye et al., 2021) (see Inline Supplementary Fig. 1). The funnel-tip method also allows for the automated delineation of approximate rostral-caudal sections within the LC, potentially increasing sensitivity and specificity to disintegrity (Liu et al., 2017). We have previously employed the funnel-tip method to capture LC degeneration in Alzheimer's disease (Cassidy et al., 2022), though note that some parameters (e.g., number of LC sections, number of adjacent voxels identified per slice) vary as a consequence of the differing NM-MRI acquisitions.

2.4.3. Image processing

We used FSL (FMRIB Software Library, Oxford University, UK) to register and average each participant's four NM-MRI measurements into a combined image. All subsequent steps in our 10-step pipeline were performed using default DARTEL routines in SPM12 (Wellcome Trust, London, UK): (1) Coregister each participant's combined NM image, and T2, to their T1; (2) Spatially normalize each participant's combined NM image, T1, and T2 to Montreal Neurological Institute (MNI) standardized space; (3) Generate a study-specific "template" image, by averaging together normalized NM images from all participants; (4) Manually draw an 'over-inclusive' LC mask on the template image, including any voxel that appears to contain LC even if including another structure (e.g., ventricle), in order to ensure coverage; (5) Divide the LC mask into three rostro-middle-caudal sections, each spanning 5 mm in the z-axis; (6) Spatially deform (inverse normalize) the full and sectioned over-inclusive LC masks from standardized MNI space to the native-space combined NM image from each participant, essentially defining the borders of a personalized "LC search space"; (7) Normalize the signal intensity of each participant's combined NM image, by adjusting contrast relative to a reference region, the pons, known to contain minimal neuromelanin; (8) Identify the LC as the brightest cluster of six adjacent voxels within the "LC search space", on each side and slice of each participant's thresholded combined NM image; (9) Ascribe the LC voxels on each side and slice to one of the three rostro-caudal sections based on their overlap with the divided overinclusive LC mask; (10) Calculate six contrast ratios for each participant (one for each of three rostral-caudal sections, in both hemispheres), which we interpreted as an in vivo measure of LC integrity (Keren et al., 2015). Specifically, contrast ratio was calculated as the relative difference in the mean signal intensity across the six adjacent voxels ($SI\overline{x}_6$) from the signal intensity of a circle (r = 12 mm) placed in the pons reference region (RR) in the same slice: contrast ratio = $(SI\overline{x}_6 - mode(SI_{RR}))/mode(SI_{RR})$. We utilized the modal pons value so as to mitigate the influence of extreme intensity values. Select steps are visualized in Fig. 1, and contrast ratio values are reported in Inline Supplementary Table 4. Quality control of step 8 revealed all segmentations plausible (implausible segmentations might

[A] LC-MRI   [B] Over-inclusive LC mask   [C] LC segmentation   [D] Pons reference

[E] Rostral-caudal sections
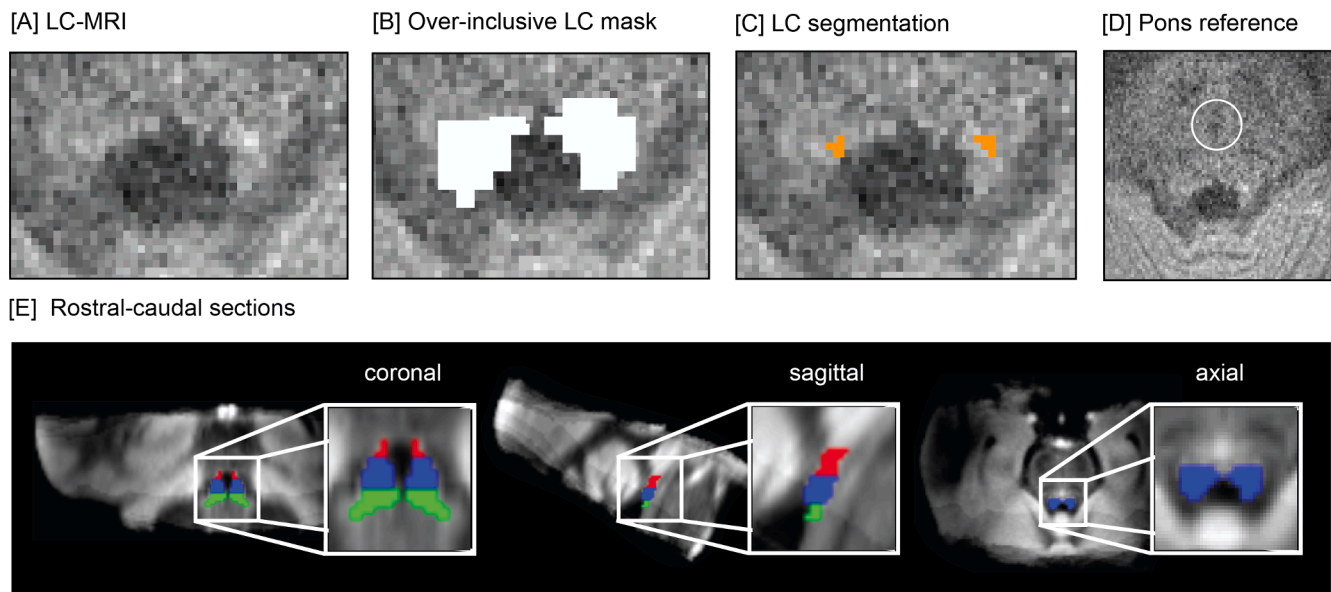
coronal   sagittal   axial

Fig. 1. Semi-automated LC segmentation. [A] Normalized NM-MRI image from an example participant (LLD), in native space. [B] The manually-drawn over-inclusive mask (white) projected to the example participant's NM image [preprocessing step **6**]. [C] Automatic identification of the LC (orange) within the over-inclusive mask search space, defined as the brightest cluster of 6 adjacent voxels [preprocessing step **8**]. [D] the pons reference region (white). [E] The rostral (red), middle (blue), and caudal (green) sections of the manually-drawn over-inclusive mask.

place the LC in or partially in the fourth ventricle as a consequence of a bright artifact) and mostly contiguous across slices, and thus manual correction was not required. Inline Supplementary Fig. 2 shows the segmentation for a randomly selected LLD participant, across all slices and all planes, and Inline Supplementary Fig. 3 shows the segmentation for 12 randomly selected participants in the axial view.

2.5. Statistical analysis

We performed all statistical analyses in R 4.0.5 (R Core Team, 2021). The distributions of all variables (including LC relative contrast) were normal, with the exception of cognitive scores, which were transformed (via arcsine). All statistical tests were evaluated at alpha = 0.05, and included adjustment for age and/or sex, unless age or sex was the variable of primary interest. We performed two-sided *t*-tests with equal variances not assumed for all group comparisons, and ANOVAs for all comparisons across LC sections, followed by Tukey post-hoc testing as required. We examined independent and interactive effects of diagnosis and age on LC-MRI contrast ratios via linear regression. As a consequence of the unanticipated null effect of diagnosis and age on LC integrity, we opted to investigate multivariate relationships between our six LC and fourteen cognition measurements, across the combined LLD and ND sample, using canonical correlation analysis (CCA) (Hotelling 1936); see (Wang et al., 2020) for an excellent primer. The driving motivation to use CCA was that, as a "doubly multivariate" method, it affords "many-to-many" comparisons beyond the "many-to-one" allowed by multiple regression, which better mimics the complexity of brain-behaviour relationships whilst also negating the need for multiple comparison correction (Sherry and Henson 2005; Wang et al., 2020). Of interest to us were the CCA model's canonical correlation value (R_c), which indicates the shared correlation structure between canonical variates, as well as its structure coefficients (r_s) (sometimes termed 'canonical loadings'), which provide a measure of within-set variable-to-variate correlation, and provide insight into the importance of each observed feature to the CCA solution. We measured stability of structure coefficients via a leave-one-participant-out jackknife procedure (Miller 1974; Dinga et al., 2019). Because our sample size falls short of the 5:1 observation-to-feature ratio minimally recommended for CCA analysis (Tabachnick et al., 2007) (ours is 48:20, roughly 2.5:1), our CCA should

be interpreted as merely exploratory to the end of informing future hypothesis-driven research.

3. Results

3.1. Participant characteristics

Participants in the LLD and ND groups did not differ on demographic characteristics or cognitive status, as measured by education-adjusted MoCA scores (Nasreddine et al., 2005). An equal number of participants in both groups (4 LLD and 4 ND, ~17 % of the sample,) had a MoCA score $\leq$ 24, which we took to be suggestive of possible mild cognitive impairment (MCI) (Carson et al., 2018). By design, there were significant group differences on all depression-relevant clinical assessments, including the clinician-administered Montgomery-Asberg Depression Rating Scale (MADRS) (Montgomery and Asberg 1979), but not tests of cognitive performance, measured by the RBANS (Randolph et al., 1998) and the D-KEFS (Delis, 2001). Participant demographic information, clinical characteristics, and cognitive scores are reported in Table 1.

3.2. LC-MRI characteristics

Signal intensity in the pons reference region did not differ between LLD and ND groups ($t(43.57) = 1.29$, $p = .20$, $d = 0.37$). Consistent with prior studies, LC-MRI contrast ratios were not homogeneous along the rostral-caudal axis (Ye et al., 2021; Betts et al., 2017). Both LLD and ND participants showed near-identical patterns, whereby the middle section had higher contrast than the rostral section, and both middle and rostral sections showed higher contrast than the caudal section, when analyzed separately by hemisphere (six sections) (Fig. 2A) and jointly within hemisphere (three bilateral sections) (Inline Supplementary Fig. 4). This pattern agrees with a histological study that reported a dense packing of noradrenergic cells in a thin central LC compartment and dispersion towards rostral and especially caudal extremities (Fernandes et al., 2012).
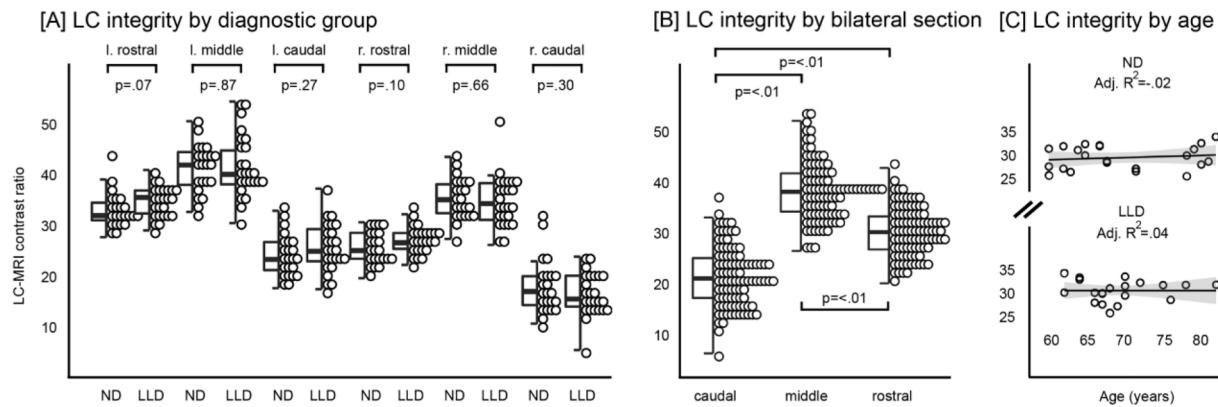
Fig. 2. LC integrity by diagnosis, section, and age. The hybrid plots [A-B] show the five-number summary (boxplot, left), and observed data (dotplot, right). [A] Uncorrected two-tailed t-tests revealed no diagnostic group difference in relative LC contrast, in any of the six sections. However, ANOVA revealed that LC contrast ratio values differ between all sections, with Tukey post-hoc testing revealing a difference in all comparisons except left caudal and right middle (results not shown; p = <.001 in the combined ND-LLD group). [B] ANOVA revealed strong evidence of differential relative contrast along the rostral-caudal axis. (Note that this plot shows average values and combines data from LLD and comparison groups, but the same effect was observed in each group, respectively; for visualization by group, see Supplementary Fig. 4.) [C] LC contrast ratio values were not associated with age in the LLD nor ND group. Average contrast ratio is shown.

3.3. LC integrity, diagnosis, and age

Contrary to our expectations, participants with LLD (M = 30.35, SD = 3.26) and ND comparisons (M = 29.86, SD = 2.85) showed comparable MR-indexed integrity across the entire LC extent, ($F(1,46)$ = −0.29, p =.59, d = Fig. 2A), and within each section (see Inline Supplementary Table 4 for section-specific statistics). In a post-hoc analysis, we confirmed that LC integrity showed no significant correlation with depressive symptom severity, as captured by the MADRS (r(46) = 0.15, p =.29) and Patient Health Questionnaire (Kroenke, Spitzer, and Williams 2001) (PHQ-9, r(46) = 0.04, p =.77). We observed no linear association between age and integrity across the combined LLD and ND comparison group, r(46) = −0.21, p =.14, nor an interaction between diagnosis and age, R^2 = 0.07, $F(3,44)$ = 1.12, p =.40. There were no sex differences in integrity in either group.

3.4. LC integrity and cognition

Because we found no diagnostic nor age effect on LC integrity, we proceeded to explore associations with cognition across the combined LLD and ND sample. Raw correlations between all LC and cognition

variables provided to the CCA are shown in Inline Supplementary Fig. 5. The full CCA model, assessing the relationship across the six derived variates, showed a high canonical correlation of R_c = 0.85 (Fig. 3A), and explained 95.9% of variance across sets. The full model was significant compared to the parametric F distribution, Wilks' lambda = 0.04, $F(84, 162.44)$ = 1.59, p =.01. We confirmed model significance via permutation testing (1000 permutations), p =.01 (Fig. 3B). Innate hierarchical significance testing revealed only the first canonical variate pair (CV1) to be significant, which itself explained 72.83% of variance shared between derived variates. We elected to interpret features as 'important' if they showed a structure coefficient (r_s) value of ≥|0.35|. On this basis, CV1 showed high contributions from the left caudal (r_s = −0.478) and right rostral (r_s = 0.366) LC, as well as RBANS Attention (r_s = 0.355) and Delayed memory (r_s = 0.399), along with D-KEFS Trail Making Test: Numbers (r_s = −0.371) and Verbal fluency: Letters (r_s = −0.395) (Fig. 3C). Feature importance estimates for all observed variables were relatively stable under jackknife participant-wise deletion (Fig. 3D), with small mean differences between the model and resampled structure coefficients, and low dispersion within the resampled structure coefficients (Inline Supplementary Table 5). To confirm that the identified multivariate relationship between LC integrity and cognition was
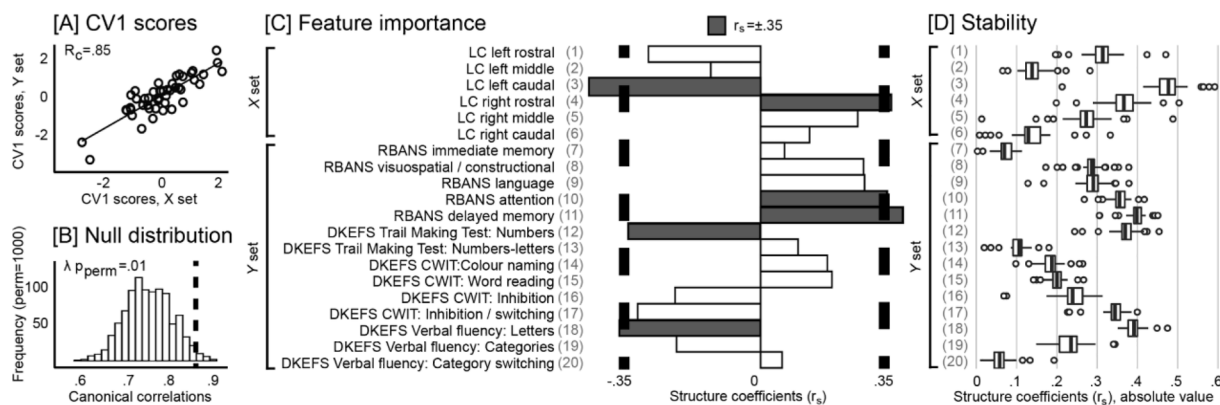

Fig. 3. Exploratory CCA links LC integrity and cognition. [A] Individual participant scores (one point per participant), for the first and only significant canonical variate, CV1. Participant scores underlie the canonical correlation, R_c. [B] The null distribution of canonical correlations for CV1, obtained via bootstrapped resampling with replacement. [C] Standardized structure coefficients ('canonical loadings') for CV1. Observed variables passing the threshold of $r_{s≥}|0.35|$ are indicated in dark gray. Note that the two D-KEFS Trail Making Test scores and the four D-KEFS Colour-Word Interference Test scores are time-to-completion (seconds); thus, lower scores are better. [D] Stability of structure coefficients was assessed in-sample via a delete-one jackknife procedure. Absolute values are shown for ease of comparison. Though some participants wielded outsized effects on structure coefficient estimates (visualized as outliers), mean differences between the model and resampled estimates were low, as was dispersion (standard deviation) of resampled estimates.

independent of diagnosis, we confirmed that LLD and ND participants showed indistinguishable correlations between X and Y scores in CV1 variate space (as depicted in Fig. 3A, z = 1.35, p =.18). Further, CV1 X and Y set scores were not associated with depression severity, as measured by the MADRS ($r_X(46) = -0.19$, $p =.2$; $r_Y(46) = -0.2$, $p =.17$) and PHQ-9 ($r_X(46) = -0.19$, $p =.2$; $r_Y(46) = -0.18$, $p =.22$).

4. Discussion

In this study, we acquired NM-MRI from older adults aged > 60, including 25 individuals with LLD and 23 cognitively-matched ND comparisons. We segmented the rostral-caudal extent of the LC via a semi-automated "funnel-tip" method, and interpreted relative contrast estimates as an in vivo proxy of integrity. Then, we examined associations between integrity and diagnosis, age, and cognition.

Contrary to our primary hypothesis, we found no significant LC-MRI relative contrast attenuation in LLD compared to ND comparison participants, suggesting that depression in late-life might not undermine LC integrity in a way that is distinct from variability in normal aging. Three prior studies did report compromised LC integrity in individuals with depression relative to controls (Guinea-Izquierdo et al., 2021; Shibata et al., 2008, 2007). Importantly, however, participants in those studies were either younger (<65 years old, average age 44.6) (Shibata et al., 2008) or spanned the entire adult age range (22–83, average age 49.1) (Shibata et al., 2007). It is possible that differences are less detectable in late life due to age-dependent disintegrity (Shibata et al., 2006), or higher intraindividual variability (Liu et al., 2019). To the best of our knowledge, Guinea-Izquierdo and colleagues (2021) report the only prior LC-MRI study specific to LLD, and this group found lower relative contrast was limited to those taking serotonin/norepinephrine reuptake inhibitors (SNRIs): individuals with LLD not taking SNRIs were indistinguishable from age-matched comparison participants. As SNRIs inhibit norepinephrine reuptake, increased levels in the synaptic cleft could lead to a decrease in intracellular norepinephrine synthesis and metabolism, which, if sustained over time, could result in decreased neuromelanin accumulation in the LC. Hence, the low number of participants taking noradrenergic medication could partially explain why we did not observe a similar pattern in our study.

Another possibility is that our relatively small sample size may have impacted our ability to find statistical significance. However, power calculations using previously reported effect sizes (Shibata et al., 2007) indicated our sample size to be sufficiently powered (>0.8) to detect differences in the LC's entire extent, and medial and rostral sections (Cohen's d = 0.99 and 0.71, respectively), though not the caudal section (d = 0.11). A promising avenue for future research would be to evaluate whether pathological anxiety, often comorbid with depression, might counteract the purported signal-attenuating effects of depression on LC-MRI. In support of this notion, in rodents, chronic and repeated stress results in increased LC norepinephrine (Fan et al., 2014), and one LC-MRI study in humans report a statistical trend towards increased LC contrast in individuals with anxiety compared to healthy controls (Morris et al., 2020).

Also contrary to our expectation, our analysis examining the relationship between LC integrity and age did not reveal a linear effect of age across the entire LC extent nor its sections. This was so in each of the LLD and ND groups, as well as their combination. This null result is perhaps not surprising, given our study's age range of 60–85, and that the purported "inverted U-shape" of LC integrity over chronological age peaks at about age 60, and then appears to plateau or only slightly decrease in healthy individuals (Shibata et al., 2006; Liu et al., 2019). Our null result is in keeping with a large lifespan study of cognitively normal adults that reported stable LC contrast above the age of 57 (Liu et al., 2020a; Liu et al., 2019). Our results are also consistent with a recent postmortem analysis of healthy adults, which found no age-related reduction in LC cell count (Theofilas et al., 2017).

Because we observed no diagnostic effect, we combined LLD and ND participants in a single, larger group to explore multivariate associations between MR-indexed LC integrity and cognition. Our CCA identified a strong, significant relationship between integrity and cognitive performance, consistent with past evidence suggesting that the LC undergirds cognition in healthy older adults (Dahl et al., 2019; Hämmerer et al., 2018; Liu et al., 2020b; Elman et al., 2020; Clewett et al., 2016), and tentatively extending this association to include individuals with LLD. Examination of feature importance via structure coefficients suggested spatially-differentiated contributions from the left caudal and right rostral LC and four cognitive domains/tasks (RBANS Attention and Delayed memory, and D-KEFS Trail Making Test: Numbers and Verbal fluency: Letters). Better cognitive performance was associated with higher integrity in the right rostral LC (except for Verbal fluency: Letters) but lower integrity in the left caudal LC.

Two patterns from our exploratory CCA warrant future investigation via hypothesis-driven research. The first is the apparent inverse contribution to CV1 held by the right rostral and left caudal LC. The positive contribution shown by the rostral LC is broadly consistent with prior work showing univariate associations between rostral LC integrity and long-term memory function (Dahl et al., 2019), and the performance on both norepinephrine-dependent and -independent cognitive tasks, in healthy older adults (Liu et al., 2020b). To the best of our knowledge, no study has reported an association between caudal LC and cognition. However, one recent study investigating relative contrast and cortical thickness found markedly different associations as a function of LC topology: in younger adults, relative contrast in rostral LC positively correlated with cortical thickness, whereas the caudal LC showed a negative relationship (Bachman et al., 2021). Though LC topology is far from established, the rostral section demonstrates more widespread connectivity to cortex (Schwarz and Luo, 2015), and thus may prove more integral to cognitive performance. Future multimodal work, jointly investigating LC disintegrity and dysfunction (Clewett et al., 2018; Mather et al., 2020), ideally at ultra-high field, should further probe section-wise differentiation. Alternatively, it is possible that MR-indexed integrity may be less accurate in the caudal LC, as this section is more diffusely organized compared to the rostral and middle sections (Schwarz and Luo, 2015).

A second curious pattern evident in the CCA is the negative contribution to CV1 shown by D-KEFS Verbal fluency: Letters task. This mirrors the surprising negative bivariate correlation between this task and LC integrity (and all verbal fluency measures, as illustrated in Inline Supplementary Fig. 5). To the best of our knowledge, the relationship between verbal fluency and LC integrity and/or the norepinephrine system has not been thoroughly explored, though one study failed to find an association between processing speed as measured by the Digit Symbol task and NM-MRI relative contrast in the substantia nigra (Wengler et al., 2020a). Further work is needed to clarify if some domains of cognitive performance may be independent of, or negatively correlated with LC integrity.

Our study is strengthened by our robust estimation of relative LC contrast. Unlike several prior studies that acquired a T1-weighted turbo spin-echo (TSE) pulse sequence with an incidental MT pulse, we acquired a GRE sequence with an explicit MT pulse. Several methodological studies have now shown that GRE MT sequences generate higher and more reliable signal measurements than comparable TSE sequences (Chen et al., 2014; Priovoulos et al., 2018; van der Pluijm et al., 2021), perhaps because the NM-MRI contrast reflects MT effects (Keren et al., 2015; Trujillo et al., 2017). Moreover, our semi-automated "funnel-tip" segmentation method, operating over unprocessed LC-MRI images in native space, minimizes opportunity for distortion of the tiny nucleus (Cassidy et al., 2022) (but see (Giorgi et al., 2022a,b) for a recent comparison of native space to MRI template space). The total success of our method in identifying plausible LC largely eliminates the human bottleneck of structural segmentation, and opens the prospect of future clinical use.

Our findings should be considered in light of several limitations.

Perhaps most notable are limitations with our sample. Although adequately powered to detect effects of diagnosis based on previously reported sizes, our sample was relatively small, which raises the risk of both Type I and Type II errors. Our sample did not include the elderly over 85 years, reflecting difficulties recruiting participants in that age range. The LLD group consisted of mostly women, in whom depression is more commonly diagnosed (Luijendijk et al., 2008). The LLD group was composed mostly of those with recurrent depression (n = 17), but also those who reported a single past episode (n = 5) and/or were experiencing a first-episode (n = 3); these subgroups may have distinct cognitive characteristics. Moreover, 16.67 % of our sample had possible MCI, which we defined as a MoCA score $\leq$ 24 (note that had we employed a $\leq$ 26 cutoff, consistent with the original MoCA paper, 52.01 % of our sample would have possible MCI, though still with equal proportions of LLD and ND). Though a previous study found no effect of MCI on LC-MRI (Betts et al., 2019), it is possible that participants in our sample were in fact presymptomatic for pathological conditions such as Alzheimer's disease.

Several limitations also pertain to our methods. First, LC-MRI remains an active area of development, and faces challenges intrinsic to measuring a subcortical nucleus in vivo. At 3T spatial resolution, measurement of LC contrast ratio may be subject to partial volume effects, in which LC voxels contain non-LC tissue. Our acquisition had a particularly large slice thickness, which improves signal-to-noise and decreases scan duration, but increases the likelihood of partial volume effects. Moreover, though we adjusted LC contrast relative to a reference region, it remains possible that integrity estimates partially reflect between-participant fluctuations in intensity scaling. Future studies using quantitative MRI, ideally at 7T, may avoid this concern. Though our decision to localize the LC in native space obviates registration error, it does allow for inconsistencies in field-of-view across subjects, which may slightly impact our relative contrast estimates in the rostral and caudal LC. Second, we must again emphasize cautious interpretation of our exploratory results. CCA is prone to instability, especially in light of low observation-to-feature ratios, and ours is approximately half of the typical standard of 5:1 (Tabachnick et al., 2007). Though our jackknife procedure suggested stability, leave-one-participant-out is admittedly a mild perturbation. In an independent sample, it remains likely feature importance estimates would vary (Barcikowski and Stevens, 1975; Thorndike and Weiss, 1973), and that the observed large canonical correlation would be lower (Le Floch et al., 2012). Future studies with larger samples, that afford higher observation-to-feature ratios and external validation, are required to confirm our preliminary exploration, and better parse multivariate relationships between LC integrity and cognition. Lastly, because our CCA included the RBANS and D-KEFS in their entirety, without consideration of the relationship between particular tasks and the norepinephrine system, we are unable to determine if high contributions to CV1 reflect the role of norepinephrine in the cognitive domain in question, beyond attention and arousal that generally underlies cognitive performance (Liu et al., 2020b).

In conclusion, we did not find any difference in MR-indexed LC integrity between cognitively-matched older adults with and without LLD, or as a function of age, suggesting that, contrary to our initial hypothesis, LC integrity may be relatively preserved in LLD. Further, our exploratory multivariate analysis that combined LLD and ND groups, suggests that individual differences in LC integrity are cognitively relevant; this is consistent with the known involvement of LC norepinephrine in cognition in healthy older adults, and tentatively extends it for the first time to individuals with LLD. Taken together, our results provide a rationale for future research investigating LC integrity as a biomarker of cognition in a broad array of neurological and psychiatric disorders that involve cognitive impairment, and/or depression as a comorbidity.

Disclosures

CMC is an inventor on a patent using the analysis method described here, licensed to Terran Biosciences, but has received no royalties. The other authors report no conflicts of interest.

CRediT authorship contribution statement

Navona Calarco: Conceptualization, Data curation, Formal analysis, Methodology, Validation, Visualization, Writing – original draft. **Clifford M. Cassidy:** Methodology, Software, Supervision, Validation. **Ben Selby:** Data curation, Formal analysis, Validation. **Colin Hawco:** Software, Validation. **Aristotle N. Voineskos:** Funding acquisition, Investigation, Resources, Software. **Breno S. Diniz:** Funding acquisition, Investigation. **Yuliya S. Nikolova:** Conceptualization, Formal analysis, Funding acquisition, Investigation, Methodology, Project administration, Resources, Supervision, Visualization, Writing – original draft.

Declaration of Competing Interest

The authors declare that they have no known competing financial interests or personal relationships that could have appeared to influence the work reported in this paper.

Data availability

The authors do not have permission to share data.

Appendix A. Supplementary data

Supplementary data to this article can be found online at https://doi.org/10.1016/j.nicl.2022.103182.

References

Anand, A., Charney, D.S., 2000. Norepinephrine dysfunction in depression. J. Clin. Psychiatry 61 (Suppl 10), 16–24.

Bachman, S.L., Dahl, M.J., Werkle-Bergner, M., Düzel, S., Forlim, C.G., Lindenberger, U., Kühn, S., Mather, M., 2021. Locus coeruleus MRI contrast is associated with cortical thickness in older adults. Neurobiol. Aging 100 (April), 72–82.

Barcikowski, R.S., Stevens, J.P., 1975. A Monte Carlo study of the stability of canonical correlations, canonical weights and canonical variate-variable correlations. Multivar. Behav. Res. 10 (3), 353–364.

Beardmore, R., Hou, R., Darekar, A., Holmes, C., Boche, D., 2021. The locus coeruleus in aging and Alzheimer's disease: A postmortem and brain imaging review. J. Alzheimers Dis. https://doi.org/10.3233/jad-210191.

Betts, M.J., Cardenas-Blanco, A., Kanowski, M., Jessen, F., Düzel, E., 2017. In vivo MRI assessment of the human locus coeruleus along its rostrocaudal extent in young and older adults. NeuroImage 163 (December), 150–219.

Betts, M.J., Cardenas-Blanco, A., Kanowski, M., Spottke, A., Teipel, S.J., Kilimann, I., Jessen, F., Düzel, E., 2019. Locus coeruleus MRI contrast is reduced in Alzheimer's disease dementia and correlates with CSF Aβ levels. Alzheimers Dementia 11 (December), 281–325.

Byers, A.L., Yaffe, K., 2011. Depression and risk of developing dementia. Nature Rev. Neurol. 7 (6), 323–331.

Carson, N., Leach, L., Murphy, K.J., 2018. A re-examination of montreal cognitive assessment (MoCA) cutoff scores. Int. J. Geriatr. Psychiatry 33 (2), 379–388.

Cassidy, C.M., Therriault, J., Pascoal, T.A., Cheung, V., Savard, M., Tuominen, L., Chamoun, M., et al., 2022. Association of locus coeruleus integrity with Braak stage and Neuropsychiatric symptom severity in Alzheimer's disease. Neuropsychopharmacology. https://doi.org/10.1038/s41386-022-01293-6.

Chamberlain, S.R., Robbins, T.W., 2013. Noradrenergic modulation of cognition: therapeutic implications. J. Psychopharmacol. 27 (8), 694–718.

Chan-Palay, V., Asan, E., 1989. Quantitation of catecholamine neurons in the locus coeruleus in human brains of normal young and older adults and in depression. J. Comp. Neurol. 287 (3), 357–372.

Chen, X., Huddleston, D.E., Langley, J., Ahn, S., Barnum, C.J., Factor, S.A., Levey, A.I., Xiaoping, H.u., 2014. Simultaneous imaging of locus coeruleus and substantia nigra with a quantitative neuromelanin MRI approach. Magn. Reson. Imaging 32 (10), 1301–1306.

Clewett, D.V., Lee, T.-H., Greening, S., Ponzio, A., Margalit, E., Mather, M., 2016. Neuromelanin marks the spot: identifying a locus coeruleus biomarker of cognitive reserve in healthy aging. Neurobiol. Aging 37 (January), 117–126.

Clewett, D.V., Huang, R., Velasco, R., Lee, T.-H., Mather, M., 2018. Locus coeruleus activity strengthens prioritized memories under arousal. J. Neurosci. 38 (6), 1558–1574.

Cottingham, C., Wang, Q., 2012. A2 adrenergic receptor dysregulation in depressive disorders: implications for the neurobiology of depression and antidepressant therapy. Neurosci. Biobehav. Rev. 36 (10), 2214–2225.

Dahl, M.J., Mather, M., Düzel, S., Bodammer, N.C., Lindenberger, U., Kühn, S., Werkle-Bergner, M., 2019. Rostral locus coeruleus integrity is associated with better memory performance in older adults. Nat. Hum. Behav. 3 (11), 1203–1214.

Dahl, M.J., Mather, M., Werkle-Bergner, M., Kennedy, B.L., Guzman, S., Hurth, K., Miller, C.A., et al., 2022. Locus coeruleus integrity is related to tau burden and memory loss in autosomal-dominant Alzheimer's disease. Neurobiol. Aging 112 (April), 39–54.

Delis, D.C., 2001. Delis - Kaplan Executive Function System: Examiners Manual. Psychological Corporation.

Dinga, Richard, Lianne Schmaal, Brenda W. J. H. Penninx, Marie Jose van Tol, Dick J. Veltman, Laura van Velzen, Maarten Mennes, Nic J. A. van der Wee, and Andre F. Marquand. 2019. Evaluating the Evidence for Biotypes of Depression: Methodological Replication and Extension of Drysdale et al. (2017). *NeuroImage: Clin.* 22 (January): 101796.

Elman, J.A., Puckett, O.K., Beck, A., Panizzon, M.S., Sanderson-Cimino, M.E., Gustavson, D.E., Lyons, M.J., Franz, C.E., Kremen, W.S., 2020. MRI-assessed locus coeruleus integrity is heritable and associated with cognition, Alzheimer's risk, and sleep-wake disturbance. Alzheimers Dementia. https://doi.org/10.1002/alz.044862.

Fan, Y., Chen, P., Li, Y., Cui, K., Noel, D.M., Cummins, E.D., Peterson, D.J., Brown, R.W., Zhu, M.-Y., 2014. Corticosterone administration up-regulated expression of norepinephrine transporter and dopamine β-hydroxylase in rat locus coeruleus and its terminal regions. J. Neurochem. 128 (3), 445–458.

Fernandes, P., Regala, J., Correia, F., Gonçalves-Ferreira, A.J., 2012. The human locus coeruleus 3-D stereotactic anatomy. Surg. Radiol. Anat. 34 (10), 879–885.

Floch, L.e., Edith, V.G., Frouin, V., Pinel, P., Lalanne, C., Trinchera, L., Tenenhaus, A., et al., 2012. Significant correlation between a set of genetic polymorphisms and a functional brain network revealed by feature selection and sparse partial least squares. NeuroImage 63 (1), 11–24.

García-Lorenzo, Daniel, Clarisse Longo-Dos Santos, Claire Ewenczyk, Smaranda Leu-Semenescu, Cecile Gallea, Graziella Quattrocchi, Patricia Pita Lobo, et al. 2013. The coeruleus/subcoeruleus complex in rapid eye movement sleep behaviour disorders in Parkinson's disease. *Brain* 136 (Pt 7): 2120–2129.

Giorgi, F.S., Lombardo, F., Galgani, A., Hlavata, H., Latta, D.D., Martini, N., Pavese, N., et al., 2022a. Locus coeruleus magnetic resonance imaging in cognitively intact elderly subjects. Brain Imaging and Behavior 16 (3), 1077–1087.

Giorgi, F.S., Martini, N., Lombardo, F., Galgani, A., Bastiani, L., Della Latta, D., Hlavata, H., et al., 2022b. Locus coeruleus magnetic resonance imaging: A comparison between native-space and template-space approach. J. Neural Transm. 129 (4), 387–394.

Guinea-Izquierdo, A., Giménez, M., Martínez-Zalacaín, I., Del Cerro, I., Canal-Noguer, P., Blasco, G., Gascón, J., et al., 2021. Lower locus coeruleus MRI intensity in patients with late-life major depression. PeerJ 9 (February), e10828.

Hämmerer, D., Callaghan, M.F., Hopkins, A., Kosciessa, J., Betts, M., Cardenas-Blanco, A., Kanowski, M., et al., 2018. Locus coeruleus integrity in old age is selectively related to memories linked with salient negative events. Proc. Natl. Acad. Sci. U. S. A. 115 (9), 2228–2233.

Hotelling, H., 1936. Relations between two sets of variates. Biometrika. https://doi.org/10.2307/2333955.

Jacobs, H.I.L., Becker, J.A., Kwong, K., Engels-Domínguez, N., Prokopiou, P.C., Papp, K.V., Properzi, M., et al., 2021. In vivo and neuropathology data support locus coeruleus integrity as indicator of Alzheimer's disease pathology and cognitive decline. Sci. Transl. Med. 13 (612), eabj2511.

Kelberman, M., Keilholz, S., Weinshenker, D., 2020. What's that (blue) spot on my MRI? Multimodal neuroimaging of the locus coeruleus in neurodegenerative disease. Front. Neurosci. https://doi.org/10.3389/fnins.2020.583421.

Keren, N.I., Lozar, C.T., Harris, K.C., Morgan, P.S., Eckert, M.A., 2009. In vivo mapping of the human locus coeruleus. NeuroImage 47 (4), 1261–2127.

Keren, N.I., Taheri, S., Vazey, E.M., Morgan, P.S., Granholm, A.-C., Aston-Jones, G.S., Eckert, M.A., 2015. Histologic validation of locus coeruleus MRI contrast in post-mortem tissue. NeuroImage 113 (June), 235–245.

Kroenke, K., Spitzer, R.L., Williams, J.B., 2001. The PHQ-9: validity of a brief depression severity measure. J. Gen. Intern. Med. 16 (9), 606–613.

Langley, J., Huddleston, D.E., Liu, C.J., Xiaoping, H., 2017. Reproducibility of locus coeruleus and substantia nigra imaging with neuromelanin sensitive MRI. Magma 30 (2), 121–215.

Liu, Kathy Y., Julio Acosta-Cabronero, Arturo Cardenas-Blanco, Clare Loane, Alex J. Berry, Matthew J. Betts, Rogier A. Kievit, et al. 2020. Corrigendum to In vivo visualization of age-related differences in the locus coeruleus. Neurobiology of Aging Volume 74, February 2019, Pages 101-111. *Neurobiol. Aging* 91 (July): 172–174.

Liu, K.Y., Marijatta, F., Hämmerer, D., Acosta-Cabronero, J., Düzel, E., Howard, R.J., 2017. Magnetic resonance imaging of the human locus coeruleus: A systematic review. Neurosci. Biobehav. Rev. 83 (December), 325–355.

Liu, K.Y., Acosta-Cabronero, J., Cardenas-Blanco, A., Loane, C., Berry, A.J., Betts, M.J., Kievit, R.A., et al., 2019. In Vivo Visualization of Age-Related Differences in the Locus Coeruleus. Neurobiol. Aging 74 (February), 101–111.

Liu, K.Y., Kievit, R.A., Tsvetanov, K.A., Betts, M.J., Düzel, E., Rowe, J.B., Cam-CAN, R.H., Hämmerer, D., 2020. Noradrenergic-dependent functions are associated with age-related locus coeruleus signal intensity differences. Nat. Commun. 11 (1), 1712.

Luijendijk, H.J., van den Berg, J.F., Dekker, M.J.H.J., van Tuijl, H.R., Otte, W., Smit, F., Hofman, A., Stricker, B.H.C., Tiemeier, H., 2008. Incidence and recurrence of late-life depression. Arch. Gen. Psychiatry 65 (12), 1394–1401.

Mather, M., Huang, R., Clewett, D., Nielsen, S.E., Velasco, R., Kristie, T.u., Han, S., Kennedy, B.L., 2020. Isometric exercise facilitates attention to salient events in women via the noradrenergic system. NeuroImage 210 (April), 116560.

Miller, R.G., 1974. The jackknife-a review. Biometrika 61 (1), 1–15.

Montgomery, S.A., Asberg, M., 1979. A new depression scale designed to be sensitive to change. Br. J. Psychiatry 134 (April), 382–439.

Morris, L.S., Tan, A., Smith, D.A., Grehl, M., Han-Huang, K., Naidich, T.P., Charney, D.S., Balchandani, P., Kundu, P., Murrough, J.W., 2020. Sub-millimeter variation in human locus coeruleus is associated with dimensional measures of psychopathology: an in vivo ultra-high field 7-Tesla MRI study. NeuroImage Clin. 25 (January), 102148.

Nasreddine, Z.S., Phillips, N.A., Bédirian, V., Charbonneau, S., Whitehead, V., Collin, I., Cummings, J.L., Chertkow, H., 2005. The Montreal Cognitive Assessment, MoCA: A brief screening tool for mild cognitive impairment. J. Am. Geriatr. Soc. 53 (4), 695–769.

Olivieri, P., Lagarde, J., Lehericy, S., Valabrègue, R., Michel, A., Macé, P., Caillé, F., Gervais, P., Bottlaender, M., Sarazin, M., 2019. Early alteration of the locus coeruleus in phenotypic variants of Alzheimer's disease. Ann. Clin. Transl. Neurol. 6 (7), 1345–1351.

Poe, G.R., Foote, S., Eschenko, O., Johansen, J.P., Bouret, S., Aston-Jones, G., Harley, C. W., et al., 2020. Locus coeruleus: A new look at the blue spot. Nat. Rev. Neurosci. 21 (11), 644–659.

Priovoulos, N., Jacobs, H.I.L., Ivanov, D., Uludağ, K., Verhey, F.R.J., Poser, B.A., 2018. High-resolution in vivo imaging of human locus coeruleus by magnetization transfer MRI at 3T and 7T. NeuroImage 168 (March), 427–436.

Priovoulos, N., van Boxel, S.C.J., Jacobs, H.I.L., Poser, B.A., Uludag, K., Verhey, F.R.J., Ivanov, D., 2020. Unraveling the contributions to the neuromelanin-MRI contrast. Brain Struct. Funct. 225 (9), 2757–2774.

Randolph, C., Tierney, M.C., Mohr, E., Chase, T.N., 1998. The Repeatable Battery for the Assessment of Neuropsychological Status (RBANS): Preliminary Clinical Validity. J. Clin. Exp. Neuropsychol. 20 (3), 310–339.

Sasaki, M., Shibata, E., Tohyama, K., Takahashi, J., Otsuka, K., Tsuchiya, K., Takahashi, S., Ehara, S., Terayama, Y., Sakai, A., 2006. Neuromelanin magnetic resonance imaging of locus ceruleus and substantia nigra in Parkinson's disease. NeuroReport 17 (11), 1215–2128.

Schwarz, L.A., Luo, L., 2015. Organization of the locus coeruleus-norepinephrine system. Curr. Biol. 25 (21), R1051–R1056.

Sheehan, D. V., Lecrubier, Y., Sheehan K. H., Amorim P., Janavs J., Weiller E., Hergueta T., Baker R., Dunbar G. C., 1998. The Mini-International Neuropsychiatric Interview (M.I.N.I.): The development and validation of a structured diagnostic psychiatric interview for DSM-IV and ICD-10. *J. Clin. Psychiatry* 59 (Suppl 20): 22–33;quiz 34–57.

Sherry, A., Henson, R.K., 2005. Conducting and interpreting canonical correlation analysis in personality research: A user-friendly primer. J. Pers. Assess. 84 (1), 37–48.

Shibata, E., Sasaki, M., Tohyama, K., Kanbara, Y., Otsuka, K., Ehara, S., Sakai, A., 2006. Age-related changes in locus ceruleus on neuromelanin magnetic resonance imaging at 3 Tesla. Magn. Reson. Med. Sci. 5 (4), 197–200.

Shibata, E., Sasaki, M., Tohyama, K., Otsuka, K., Sakai, A., 2007. Reduced signal of locus ceruleus in depression in quantitative neuromelanin magnetic resonance imaging. NeuroReport 18 (5), 415–448.

Shibata, E., Sasaki, M., Tohyama, K., Otsuka, K., Endoh, J., Terayama, Y., Sakai, A., 2008. Use of neuromelanin-sensitive MRI to distinguish schizophrenic and depressive patients and healthy individuals based on signal alterations in the substantia nigra and locus ceruleus. Biol. Psychiatry 64 (5), 401–406.

Sommerauer, M., Fedorova, T.D., Hansen, A.K., Knudsen, K., Otto, M., Jeppesen, J., Frederiksen, Y., et al., 2018. Evaluation of the noradrenergic system in Parkinson's disease: An 11C-MeNER PET and neuromelanin MRI study. Brain J. Neurol. 141 (2), 496–504.

Tabachnick, B.G., Fidell, L.S., Ullman, J.B., 2007. Using Multivariate Statistics, Vol. 5. Pearson Boston, MA.

Theofilas, P., Ehrenberg, A.J., Dunlop, S., Di Lorenzo, A.T., Alho, A.N., Leite, R.E.P., Rodriguez, R.D., et al., 2017. Locus coeruleus volume and cell population changes during Alzheimer's disease progression: A stereological study in human postmortem brains with potential implication for early-stage biomarker discovery. Alzheimers Dementia 13 (3), 236–246.

Thorndike, R.M., Weiss, D.J., 1973. A study of the stability of canonical correlations and canonical components. Educ. Psychol. Measur. 33 (1), 123–134.

Tona, K.-D., Keuken, M.C., de Rover, M., Lakke, E., Forstmann, B.U., Nieuwenhuis, S., van Osch, M.J.P., 2017. In vivo visualization of the locus coeruleus in humans: quantifying the test-retest reliability. Brain Struct. Funct. 222 (9), 4203–4217.

Trujillo, P., Summers, P.E., Ferrari, E., Zucca, F.A., Sturini, M., Mainardi, L.T., Cerutti, S., et al., 2017. Contrast mechanisms associated with neuromelanin-MRI. Magn. Reson. Med. 78 (5), 1790–1800.

van der Pluijm, M., Cassidy, C., Zandstra, M., Wallert, E., de Bruin, K., Booij, J., de Haan, L., Horga, G., van de Giessen, E., 2021. Reliability and reproducibility of

neuromelanin-sensitive imaging of the substantia nigra: A comparison of three different sequences. J. Magn. Reson. Imaging 53 (3), 712–721.

Wang, H.-T., Smallwood, J., Mourao-Miranda, J., Xia, C.H., Satterthwaite, T.D., Bassett, D.S., Bzdok, D., 2020. Finding the needle in a high-dimensional haystack: canonical correlation analysis for neuroscientists. NeuroImage 216 (August), 116745.

Watanabe, T., Tan, Z., Wang, X., Martinez-Hernandez, A., Frahm, J., 2019. Magnetic resonance imaging of noradrenergic neurons. Brain Struct. Funct. 224 (4), 1609–1625.

Wengler K., Ashinoff B.K., Pueraro E., Cassidy C.M., Horga G., Rutherford B. R. 2020. Association between neuromelanin-sensitive MRI signal and psychomotor slowing in late-life depression. *Neuropsychopharmacology*, September. https://doi.org/10.1038/s41386-020-00860-z.

Wengler, K., He, X., Abi-Dargham, A., Horga, G., 2020b. Reproducibility assessment of neuromelanin-sensitive magnetic resonance imaging protocols for region-of-interest and voxelwise analyses. NeuroImage 208 (March), 116457.

Ye, R., Rua, C., Claire O'Callaghan, P., Jones, S., Hezemans, F.H., Kaalund, S.S., Tsvetanov, K.A., et al., 2021. An in vivo probabilistic atlas of the human locus coeruleus at ultra-high field. NeuroImage 225, 117487.